Published in final edited form as:
Curr Opin Struct Biol. 2013 October ; 23(5): 725–733. doi:10.1016/j.sbi.2013.06.008.

Technological advances in site-directed spin labeling of proteins

Wayne L Hubbell, **Carlos J López**, **Christian Altenbach**, and **Zhongyu Yang**
Jules Stein Eye Institute and Department of Chemistry and Biochemistry, University of California, Los Angeles, CA 90095, United States

Abstract

Molecular flexibility over a wide time range is of central importance to the function of many proteins, both soluble and membrane. Revealing the modes of flexibility, their amplitudes, and time scales under physiological conditions is the challenge for spectroscopic methods, one of which is site-directed spin labeling EPR (SDSL-EPR). Here we provide an overview of some recent technological advances in SDSL-EPR related to investigation of structure, structural heterogeneity, and dynamics of proteins. These include new classes of spin labels, advances in measurement of long range distances and distance distributions, methods for identifying backbone and conformational fluctuations, and new strategies for determining the kinetics of protein motion.

Introduction

A golden age of protein physical science was ushered in by the advent of crystallographic methods which revealed how weak non-covalent interactions cooperated to stabilize the elaborate secondary, tertiary, and quaternary structures of proteins. But the information proved to be incomplete for elucidating molecular mechanisms underlying function which often rely on conformational flexibility, which is not directly revealed in the confines of the crystalline lattice. A second golden age is in progress and began when spectroscopic methods were developed to permit atomic scale resolution of protein structure and dynamics in solution. The most dramatic advances have come from solution NMR methods which provide residue specific information on protein dynamics. The technology continues to develop, but currently has relatively poor sensitivity, practical limitations for a general extension to membrane proteins in their native lipid environments, a limitation to short range inter-nuclear distance measurements, and is challenged for measuring dynamics on the μs time scale that may be important for function. These limitations provide a unique opportunity for site-directed spin labeling EPR (SDSL-EPR) to complement NMR, because they are the particular strengths of the EPR method, which is unconstrained by the size or complexity of the system under study.

Since the last review on SDSL in this journal [1], substantial progress has been made in site-directed mutagenesis, the chemistry and physics of the spin labels, methodology and instrumentation, and in computational methods. Excellent recent reviews documenting applications of SDSL to proteins have appeared [2–5], and the present contribution will be restricted to technological advances in the above areas for exploring the structure and dynamics of proteins with an emphasis on the last two years.

Corresponding author: Hubbell, Wayne L (HubbellW@jsei.ucla.edu, hubbellc@aol.com).

Nitroxide side chains

The common implementation of SDSL employs the disulfide-linked nitroxide side chain, designated R1, introduced via cysteine substitution mutagenesis (Figure 1a). In general, interpretation of EPR data from R1 in terms of protein structure and dynamics requires knowledge of the rotamers and internal dynamics of the side chain itself, and this information is most complete for the simple case of R1 at non-interacting solvent exposed sites in helices and loops. For R1 at such sites, crystallographic data from T4 lysozyme (summarized in [6]) and other proteins [7–8], including a membrane protein [9], and density functional calculations [10] document a ubiquitous intra-residue interaction of the disulfide with backbone atoms that defines a limited rotamer library [6] and constrains the nitroxide to an anisotropic motion, as suggested by an early model [11]. As discussed below, such sites are the key to mapping backbone dynamics in helices and loops. The conformation and dynamics of R1 in β structures are less well understood, but the first members of a rotamer library have been identified in recent crystal structures of R1 in β sheets [12,13•,14•].

One of the most popular applications of SDSL-EPR is inter-spin distance determination using pulsed dipolar (PD) spectroscopy in doubly labeled systems. To interpret inter-nitroxide distances in terms of protein structure, the spatial distribution of the nitroxide at an arbitrary site must be considered, and this is modulated by interactions with the environment. To account for the spatial distribution of R1 in experimental distance distributions, different strategies have been considered, including a rotamer library biased by interaction with the protein [15••] and MD simulations and Monte Carlo conformational searches [16•]. Comparison of these methods came to the conclusion that the rotamer library is the method of choice, and for the sites studied, the agreement with experiment was best when crystal structure rotamers were selected from the complete rotamer library [16•]. Other simpler approaches sample a large conformational space, either with no assumptions about rotamer probabilities [17] or with the option to weight the population according to the crystallographically favored rotamers [18].

Another means for dealing with the rotamer distribution of R1 is to eliminate it. With this in mind, new side chains with constrained geometry are being explored. For the cross-linked RX side chain (Figure 1b) [19–22] inter-spin distance distributions were narrow compared to R1 [20•], and for R1p (Figure 1c) proton relaxation enhancement suggested a single rotamer populated in solution [23]. Crystal structures of RX (PDB entry 3L2X) and the 4-phenyl analog of R1p (PDB entry 1ZUR) in T4 lysozyme show resolved electron densities for the entire side chain, unlike those for R1 which are resolved only to the disulfide due to internal disorder. The side chain TOPP (Figure 1d) [24] provides a fixed position of the spin in a protein, but so far is introduced by total synthesis, restricting its practical use to peptides or small proteins.

It may not always be possible to eliminate native cysteine residues in a protein for the introduction of nitroxides using sulfhydryl selective chemistry. For such case alternative nitroxide side chains K1 and T1 based on site-specific incorporation of unnatural amino acids have been introduced [25,26] (Figure 1e,f). The new side chains are more flexible than R1, but the spatial distributions are not prohibitively broad for their use in distance measurements [25].

Advances in distance determination

Low temperature PD spectroscopy

PD spectra of doubly labeled proteins are obtained either with double quantum coherence (DQC) or double electron–electron resonance (DEER, also known as PEL-DOR) [27,28•],

both conducted at cryogenic temperatures with one exception noted below. The practical range for PD distance measurement using DEER in spin labeled proteins in aqueous media is typically quoted as ≈ 17–60 Å for commercial X-band (9.5 GHz) and Q band (35 GHz) spectrometers, the latter having substantially improved sensitivity (smaller samples, shorter data collection times) [29]. Recent improvements using tailored [30•] or combined [31•] pulse sequences, or protein deuteration [32], extend the upper distance range to 80 and possibly 100 Å while reducing data collection times and improving distance resolution.

Recently, efforts have been made to develop high frequency W-band (95 GHz) DEER, driven in part by the inherently high sensitivity. However, with nitroxides, the increased sensitivity for distance measurement may be compromised by an orientation selection due to *g* factor anisotropy that becomes important at high fields for rigid labels. This has been taken as an opportunity to obtain additional information on relative nitroxide orientation for structure determination [33] with impressive experimental results [33–35], but it remains challenging to uniquely determine the five angles and their distributions needed to completely define the structure of the radical pair, even if the required distinguishable and sufficiently rigid labels can be developed [33]. Under any circumstance, structural ambiguity due to the lack of angular information can be resolved with an increased number of pairwise distance measurements. In the end, the relative merits of more mutagenesis versus complexity of analysis must be considered.

In many cases orientation selection at W band DEER is a hindrance that prohibits the realization of high sensitivity for distance measurements. This problem was overcome with the introduction of Gd pairs as spin labels [36,37], eliminating orientation selection due to the essentially isotropic g factor of Gd^{3+} The Gd^{3+} can be introduced in the side chain C1 (Figure 1g) [38••] but other side chain chelates are possible [37,39,40•]. Gd^{3+} –nitroxide pairs have also been investigated with success [39,40•], particularly when combined with a recently developed bimodal resonator for W band [41] that allows realization of the full potential of the method [38••]. Although orientation selection is reintroduced when the nitroxide is rigid, only two angles are required to describe the geometry and these can be extracted from the data combined with simple modeling. Remarkably, interspin distances of 80 Å prove to be accessible with samples of 2–3 μL at 50 μM concentration. In addition, mixed Gd^{3+} and nitroxide labels in a homodimer allowed spectroscopic selection of distances arising from interactions between mixed spin pairs, that is, Gd^{3+}/Gd^{3+} , Gd^{3+}/ nitroxide and nitroxide/nitroxide [38••,42]. Similar distance editing using Cu^{2+}/nitroxide mixed pairs in a protein was recently reported [43]. Spectroscopic distance selection may be of use in analysis of protein complexes, and the required distinct labels can be introduced in a single protein using an unnatural amino acid and cysteine pair as recently shown [40•]. Distance editing between chemically identical spins can be accomplished if the spins can be distinguished based on spin lattice relaxation times [44].

Moving toward longer range distance measurements at physiological temperature

An unresolved issue in PD spectroscopy is the effect of the freezing process, particularly the rate, on the distributions of conformational substates. Distance distributions between R1 pairs in relatively rigid parts of T4L do not appear to be strongly dependent on freezing times in the range ≈100 μs to minutes [45], but a similar study has not been conducted to evaluate the influence on the distribution of conformational substates.

For distance mapping at physiological temperatures, dipolar broadening of CW spectra in spin pairs can be used at X band, but has a rather narrow distance range (10–20 Å). Recently the dipolar line broadening approach has been extended to ≈30 Å at L-band (1–2 GHz) using non-adiabatic rapid scan (NARS) spectroscopy developed by Hyde and coworkers [46•] The method requires that the rotational diffusion of the protein be sufficiently slow to

not average a weak dipolar interaction, but this can be achieved by the use of high viscosity or immobilization of the protein on a solid support [47] and will not be an issue for membrane proteins in their native lipid environment.

In principle, PD spectroscopy can be employed at ambient temperature if the phase memory time (T_m) of the spin label is long and rotational diffusion of the protein is arrested. A step in this direction has recently been reported for a protein immobilized on a solid support by using a novel triarylmethyl (TAM) spin label (Figure 1h) and DQC spectroscopy. At present, the method is limited to short distances but can be extended by synthesis of new TAM derivatives that are predicted to have longer T_ms [48•].

Enhancement of a nitroxide T_1 relaxation by a fast relaxing paramagnetic species can be employed to measure inter-spin distances. Although typically used at cryogenic temperatures [27,49], this strategy has been employed at ambient temperatures to measure distances up to 25 Å between Cu^{2+} (the fast relaxing species) and R1 in a peptide [50]. Simulations indicate that 30–35 Å could be accessible using RX or R1p, or 40–45 Å using a TAM spin label due to the longer T_1 of these radicals compared to R1 (Z Yang *et al.*, unpublished data). Cu^{2+} can be introduced site selectively for example via an incorporated bipyridyl amino acid [51]. A disadvantage of the relaxation enhancement approach is that only an average distance is obtained, and that distance is strongly weighted toward short distances in a distribution due to the $1/r^6$ dependence. Nevertheless, T_1 enhancement at ambient and cryogenic temperature can be compared with DEER data on the same sample [52•], providing a strategy for interpreting the relaxation data and perhaps evaluating the influence of freezing on structure.

Revealing protein conformational exchange and measuring protein dynamics under physiological conditions

Figure 2 shows the characteristic time scale for two dynamic modes of proteins that are believed to have functional roles. The amplitude of such motions might be inferred from the widths of distance distributions determined from PD spectroscopy in frozen solution, but the relevant dynamics can only be accessed in liquid solution under physiological conditions. Suitable SDSL-EPR methods for this purpose are indicated in Figure 2, where the inherent time scales are compared to those for protein dynamics.

As indicated, the CW spectral lineshape reflects motion of the nitroxide in the range of correlation time 100 ps to 100 ns, which overlaps the time scale for side chain motion, fast protein backbone fluctuations, and overall rotational diffusion. The internal modes of interest can be resolved from overall protein rotation by attaching the protein to a solid support or by increasing viscosity [47]. In favorable cases, multifrequency EPR can be used to separate motions in different time domains as well as to resolve order and rate contributions to the CW lineshape [53,54]. For R1 on the surface of a helix, where the side chain internal motion is understood (see ‘Nitroxide Side Chains’), contributions from ns backbone fluctuations should be directly reflected in the CW lineshape. This contention is strongly supported by the correlation of rate and order of R1 motion with local helix packing in myoglobin; the detected motions are likely rigid body fluctuations of the helical segment to which R1 is attached [55••] (Figure 3a).

For conformational exchange in the time domain of μs–ms, the CW lineshape of R1 contains no information on the dynamics of the process. Nevertheless, the existence of exchange is confirmed by resolved components in the EPR spectrum of R1 and the response to osmolyte perturbation, as recently demonstrated in myoglobin [55••] (Figure 3b). To obtain information on exchange lifetimes in the ms range, methods that depend on the spin lattice

relaxation time (T_1) of nitroxides can be employed. These include CW saturation transfer EPR (ST-EPR) and the time-domain equivalent of pulsed electron–electron double resonance (P-ELDOR), both of which measure spatial reorientation dynamics of the nitroxide and require rotationally immobilized proteins and a rigid spin label. Recent publications document the feasibility of these methods for monitoring ms internal protein dynamics using the RX side chain (Figure 1b) [20•,21,22]. Pulsed saturation recovery (P-SR) directly measures T1, and can be used to determine exchange kinetics of a nitroxide between two states when the exchange lifetime is comparable to the difference in T_1 between the states. This direct exchange measurement does not require immobilization of the protein, and a rigid spin label is not necessary, but exchange lifetimes are limited to the range of ≈ 1–70 μs (Figure 2) [19]. Collectively, these methods provide access to a time scale difficult to access by NMR and which represents an important time scale for protein motions.

The upper limit of ≈1 ms for measuring dynamics at X-band currently set by ST-EPR can in principle be extended using perturbation-relaxation spectroscopy (Figure 2). One attractive perturbation is hydrostatic pressure, which is known to modulate the relative populations of conformational substates at equilibrium [56]. Therefore, an instantaneous jump in pressure will be followed by a relaxation to a new equilibrium state, which can be monitored in real time to provide the exchange kinetics. High pressure SDSL-EPR was recently reported, and the ability to detect and analyze pressure-dependent conformational equilibria in terms of populations and volumetric properties was demonstrated [57] (Figure 4). Pressure jumps of 1kbar in ≈1 ms have recently been achieved in an EPR system, which should allow determination of exchange times in the ms range and longer (M Lerch *et al.*, unpublished data); faster jumps should be feasible with existing technology. Another important application of high pressure in SDSL will be to populate low-lying excited states of proteins for spectroscopic study [56].

Conclusions and future developments

The strengths of SDSL-EPR have been enhanced. High sensitivity distance measurements with PD spectroscopy to 100 Å are possible, and methods for reasonably long range distances at physiological temperature are emerging. Of particular interest is the ability to measure internal dynamics of proteins under physiological conditions over the full range from ps to ms and beyond. Such measurements are typically made with nanomoles of sample for proteins of arbitrary MW and degree of complexity, and the sensitivity improves with increasing microwave frequency. Multifrequency EPR offers an elegant approach to resolving different dynamic modes in the ns time domain. The capability for monitoring slow (μs) motions at equilibrium requires rigid nitroxide side chains and immobilized proteins. The RX side chain fulfills the former requirement, but further development of rigid labels with single-site attachment would be welcome. Immobilization of proteins is emerging as a requirement for room temperature distance measurements as well as for measuring internal dynamics. An elegant approach would use an unnatural amino acid to site-selectively attach the protein to a solid support. Pressure-jump/relaxation EPR has promise to extend the time scale for measuring exchange to ms and beyond without the need for immobilization of label or protein. Finally, the long relaxation times of TAM radicals make them attractive as spin labels for future development, despite their large size.

Acknowledgments

The authors thank Evan K. Brooks, Michael Lerch, and Margaux Kreitman for helpful comments on this manuscript. This work was supported by NIH grant number: 5R01 EY005216 (C.J.L.), the JSEI training grant: 2T32EY007026-36A1 (C.J.L.) and the Jules Stein Professor Endowment (W.L.H.).

References and recommended reading

Papers of particular interest, published within the period of review, have been highlighted as:

• of special interest

•• of outstanding interest

1. Fanucci GE, Cafiso DS. Recent advances and applications of site-directed spin labeling. Curr Opin Struct Biol. 2006; 16:644–653. [PubMed: 16949813]
2. Bordignon E. Site-directed spin labeling of membrane proteins. Top Curr Chem. 2012; 321:121–157. [PubMed: 21898205]
3. Drescher M. EPR in protein science: intrinsically disordered proteins. Top Curr Chem. 2012; 321:91–119. [PubMed: 21826602]
4. McHaourab HS, Steed PR, Kazmier K. Toward the fourth dimension of membrane protein structure: insight into dynamics from spin-labeling EPR spectroscopy. Structure. 2011; 19:1549–1561. [PubMed: 22078555]
5. Klare JP, Steinhoff HJ. Spin labeling EPR. Photosynth Res. 2009; 102:377–390. [PubMed: 19728138]
6. Fleissner MR, Cascio D, Hubbell WL. Structural origin of weakly ordered nitroxide motion in spin-labeled proteins. Protein Sci. 2009; 18:893–908. [PubMed: 19384990]
7. Lillington JE, Lovett JE, Johnson S, Roversi P, Timmel CR, Lea SM. Shigella flexneri Spa15 crystal structure verified in solution by double electron electron resonance. J Mol Biol. 2011; 405:427–435. [PubMed: 21075116]
8. Gruene T, Cho MK, Karyagina I, Kim HY, Grosse C, Giller K, Zweckstetter M, Becker S. Integrated analysis of the conformation of a protein-linked spin label by crystallography, EPR and NMR spectroscopy. J Biomol NMR. 2011; 49:111–119. [PubMed: 21271275]
9. Kroncke BM, Horanyi PS, Columbus L. Structural origins of nitroxide side chain dynamics on membrane protein alpha-helical sites. Biochemistry. 2010; 49:10045–10060. [PubMed: 20964375]
10. Warshaviak DT, Serbulea L, Houk KN, Hubbell WL. Conformational analysis of a nitroxide side chain in an alpha-helix with density functional theory. J Phys Chem B. 2011; 115:397–405. [PubMed: 21162593]
11. Columbus L, Kalai T, Jeko J, Hideg K, Hubbell WL. Molecular motion of spin labeled side chains in alpha-helices: analysis by variation of side chain structure. Biochemistry. 2001; 40:3828–3846. [PubMed: 11300763]
12. Freed DM, Horanyi PS, Wiener MC, Cafiso DS. Conformational exchange in a membrane transport protein is altered in protein crystals. Biophys J. 2010; 99:1604–1610. [PubMed: 20816073]
13. Freed DM, Khan AK, Horanyi PS, Cafiso DS. Molecular origin of electron paramagnetic resonance line shapes on beta-barrel membrane proteins: the local solvation environment modulates spin-label configuration. Biochemistry. 2011; 50:8792–8803. [PubMed: 21894979] The crystal structure of the R1 side chain at two sites on the bilayer-facing surface of a transmembrane β-barrel are presented, and the structural origin of the motion analyzed in terms of the R1 rotamers and native side chain interactions; the interactions that stabilize the rotamers are distinct from those in helical proteins. Of particular interest is the dependence of the EPR spectra on the composition of the lipid bilayer, which appears to modulate the rotamer population; pulse SR EPR spectroscopy is employed to distinguish rotamer exchange from protein conformational exchange.
14. Cunningham TF, McGoff MS, Sengupta I, Jaroniec CP, Horne WS, Saxena S. High-resolution structure of a protein spin-label in a solvent-exposed beta-sheet and comparison with DEER spectroscopy. Biochemistry. 2012; 51:6350–6359. [PubMed: 22809334] Crystal structures of R1 at the solvent-exposed surface of soluble β-sheet protein reveal three distinct rotamers, one of which is rare in helical proteins. DEER spectroscopy shows that the rotamers in frozen solution are the same as those observed in the crystal structures. The side chain interactions differ from those

in helical proteins, suggesting that the relationship of R1 and backbone motions may be more complex than that for helical proteins.

15. Polyhach Y, Bordignon E, Jeschke G. Rotamer libraries of spin labelled cysteines for protein studies. Phys Chem Chem Phys. 2011; 13:2356–2366. [PubMed: 21116569] MD simulations on an isolated R1 side chain are used to generate a library of 200 rotamers. When R1 is modeled in a protein structure, the library is culled using a scaled Lennard–Jones potential to account for local interactions. From the reduced set of rotamers, an inter-spin distance distribution is computed and compared with experimental DEER data to validate a proposed structural model of the protein. Predictions based on this approach are in good agreement with data obtained on two proteins of known structure. The procedure can be implemented with an available software package (MMM).
16. Klose D, Klare JP, Grohmann D, Kay CW, Werner F, Steinhoff HJ. Simulation vs. reality: a comparison of in silico distance predictions with DEER and FRET measurements. PLoS ONE. 2012; 7:e39492. [PubMed: 22761805] Inter-spin distance distributions for pairs of R1 in a protein are simulated by MD, a Monte Carlo conformational search method (MC), and the rotamer library of Polyhach *et al.* [15••] and compared with experimental DEER data. A structurally rigid protein, where distance distributions are solely due to side chain disorder, was selected for study. The MC method and rotamer library produce the best agreement with experiment. A similar study using the MC method was done for fluorescent labels and inter-label distance data from Förster resonance energy transfer (FRET). The spatial distributions of the fluorophores were substantially broader than that for R1 and in generally poorer agreement with the simulations.
17. Hagelueken G, Ward R, Naismith JH, Schiemann O. MtsslWizard: in silico spin-labeling and generation of distance distributions in PyMOL. Appl Magn Reson. 2012; 42:377–391. [PubMed: 22448103]
18. Hatmal MM, Li Y, Hegde BG, Hegde PB, Jao CC, Langen R, Haworth IS. Computer modeling of nitroxide spin labels on proteins. Biopolymers. 2012; 97:35–44. [PubMed: 21792846]
19. Bridges MD, Hideg K, Hubbell WL. Resolving conformational and rotameric exchange in spin-labeled proteins using saturation recovery EPR. Appl Magn Reson. 2010; 37:363. [PubMed: 20157634]
20. Fleissner MR, Bridges MD, Brooks EK, Cascio D, Kalai T, Hideg K, Hubbell WL. Structure and dynamics of a conformationally constrained nitroxide side chain and applications in EPR spectroscopy. Proc Natl Acad Sci U S A. 2011; 108:16241–16246. [PubMed: 21911399] In this work, the authors determine the X-ray structure of T4 lysozyme containing the bifunctional spin label RX, compare the distance distribution between R1–R1 and RX–RX labeled proteins, and show the utility of the RX label for measuring protein motions on the functionally important μs time scale using an electron-electron double resonance experiment. This paper highlights the advantages and limitations of the RX label compared to the most commonly used R1 side chain for monitoring structure and dynamics using SDSL.
21. Rayes RF, Kalai T, Hideg K, Geeves MA, Fajer PG. Dynamics of tropomyosin in muscle fibers as monitored by saturation transfer EPR of bi-functional probe. PLoS ONE. 2011; 6:e21277. [PubMed: 21701580]
22. Moen RJ, Thomas DD, Klein JC. Conformationally trapping the actin-binding cleft of myosin with a bifunctional spin label. J Biol Chem. 2013; 288:3016–3024. [PubMed: 23250750]
23. Fawzi NL, Fleissner MR, Anthis NJ, Kalai T, Hideg K, Hubbell WL, Clore GM. A rigid disulfide-linked nitroxide side chain simplifies the quantitative analysis of PRE data. J Biomol NMR. 2011; 51:105–114. [PubMed: 21947919]
24. Stoller S, Sicoli G, Baranova TY, Bennati M, Diederichsen U. TOPP: a novel nitroxide-labeled amino acid for EPR distance measurements. Angew Chem Int Ed Engl. 2011; 50:9743–9746. [PubMed: 21898726]
25. Fleissner MR, Brustad EM, Kalai T, Altenbach C, Cascio D, Peters FB, Hideg K, Peuker S, Schultz PG, Hubbell WL. Site-directed spin labeling of a genetically encoded unnatural amino acid. Proc Natl Acad Sci USA. 2009; 106:21637–21642. [PubMed: 19995976]
26. Kálai T, Fleissner MR, Jekő J, Hubbell WL, Hideg K. Synthesis of new spin labels for Cu-free click conjugation. Tetrahedron Lett. 2011; 52:2747–2749.
27. Berliner, LJ.; Eaton, GR.; Eaton, SS. Distance Measurements in Biological Systems by EPR. New York: Kluwer Academic/Plenum Publishers; 2000.

28. Jeschke G. DEER distance measurements on proteins. Annu Rev Phys Chem. 2012; 63:419–446. [PubMed: 22404592] An excellent and comprehensive review of DEER technology, its applications, strengths, and limitations.
29. Ghimire H, McCarrick RM, Budil DE, Lorigan GA. Significantly improved sensitivity of Q-band PELDOR/DEER experiments relative to X-band is observed in measuring the intercoil distance of a leucine zipper motif peptide (GCN4-LZ). Biochemistry. 2009; 48:5782–5784. [PubMed: 19476379]
30. Borbat PP, Georgieva ER, Freed JH. Improved sensitivity for long-distance measurements in biomolecules: five-pulse double electron–electron resonance. J Phys Chem Lett. 2013; 4:170–175. [PubMed: 23301118] A 5-pulse DEER method extends the feasible range of inter-spin distance measurement to ≈80 Å without additional modification of the protein (deuteration, for example). For measurements of shorter distances, data acquisition time is greatly reduced. Instrumentation for 5-pulse DEER is available at the National Biomedical Center for Advanced ESR Technology at Cornell University, Ithaca, New York.
31. Lovett JE, Lovett BW, Harmer J. DEER-stitch: combining three-and four-pulse DEER measurements for high sensitivity, deadtime free data. J Magn Reson. 2012; 223:98–106. [PubMed: 22975240] A technique designated ‘stitch-DEER’ combines 3-pulse and 4-pulse DEER data and provides a simple and direct approach to extend the feasible range of inter-spin distances without deuteration of the protein and using commercial EPR instrumentation.
32. Ward R, Bowman A, Sozudogru E, El-Mkami H, Owen-Hughes T, Norman DG. EPR distance measurements in deuterated proteins. J Magn Reson. 2010; 207:164–167. [PubMed: 20805036]
33. Savitsky A, Dubinskii AA, Zimmermann H, Lubitz W, Mobius K. High-field dipolar electron paramagnetic resonance (EPR) spectroscopy of nitroxide biradicals for determining three-dimensional structures of biomacromolecules in disordered solids. J Phys Chem B. 2011; 115:11950–11963. [PubMed: 21879744]
34. Reginsson GW, Hunter RI, Cruickshank PA, Bolton DR, Sigurdsson ST, Smith GM, Schiemann O. W-band PELDOR with 1 kW microwave power: molecular geometry, flexibility and exchange coupling. J Magn Reson. 2012; 216:175–182. [PubMed: 22386646]
35. Tkach I, Pornsuwan S, Hobartner C, Wachowius F, Sigurdsson ST, Baranova TY, Diederichsen U, Sicoli G, Bennati M. Orientation selection in distance measurements between nitroxide spin labels at 94 GHz EPR with variable dual frequency irradiation. Phys Chem Chem Phys. 2013; 15:3433–3437. [PubMed: 23381580]
36. Potapov A, Yagi H, Huber T, Jergic S, Dixon NE, Otting G, Goldfarb D. Nanometer-scale distance measurements in proteins using Gd^{3+} spin labeling. J Am Chem Soc. 2010; 132:9040–9048. [PubMed: 20536233]
37. Gordon-Grossman M, Kaminker I, Gofman Y, Shai Y, Goldfarb D. W-Band pulse EPR distance measurements in peptides using Gd($^{3+}$)-dipicolinic acid derivatives as spin labels. Phys Chem Chem Phys. 2011; 13:10771–10780. [PubMed: 21552622]
38. Kaminker I, Tkach I, Manukovsky N, Huber T, Yagi H, Otting G, Bennati M, Goldfarb D. W-band orientation selective DEER measurements on a Gd^{3+}/nitroxide mixed-labeled protein dimer with a dual mode cavity. J Magn Reson. 2013; 227:66–71. [PubMed: 23314001] The authors demonstrate a remarkably sensitive DEER measurement in a homodimeric protein with a mixed Gd^{3+}/nitroxide spin pair. The key to the high sensitivity is a dual mode resonator at W band that allows simultaneous excitation of both spin centers, which are separated by 700 MHz at W band.
39. Lueders P, Jeschke G, Yulikov M. Double electron—electron resonance measured between Gd^{3+} ions and nitroxide radicals. J Phys Chem Lett. 2011; 2:604–609.
40. Garbuio L, Bordignon E, Brooks EK, Hubbell WL, Jeschke G, Yulikov M. Orthogonal spin labeling and Gd(III)-nitroxide distance measurements on acteriophage T4-lysozyme. J Phys Chem B. 2013:10. http://dx.doi.org/10.1021/jp401806g. This work provides the first example of ‘orthogonal spin labeling’ within a single protein to introduce two spin centers using different chemistry. The nitroxide spin label is introduced via an unnatural amino acid while a sulfhydryl reactive Gd^{3+} chelate is coupled via a substituted cysteine residue.
41. Tkach I, Sicoli G, Hobartner C, Bennati M. A dual-mode microwave resonator for double electron–electron spin resonance spectroscopy at W-band microwave frequencies. J Magn Reson. 2011; 209:341–346. [PubMed: 21333570]

42. Kaminker I, Yagi H, Huber T, Feintuch A, Otting G, Goldfarb D. Spectroscopic selection of distance measurements in a protein dimer with mixed nitroxide and Gd^{3+} spin labels. Phys Chem Chem Phys. 2012; 14:4355–4358. [PubMed: 22362220]
43. Yang Z, Kurpiewski MR, Ji M, Townsend JE, Mehta P, Jen-Jacobson L, Saxena S. ESR spectroscopy identifies inhibitory Cu^{2+} sites in a DNA-modifying enzyme to reveal determinants of catalytic specificity. Proc Natl Acad Sci USA. 2012; 109:E993–E1000. [PubMed: 22493217]
44. van Wonderen JH, Kostrz DN, Dennison C, Macmillan F. Refined distances between paramagnetic centers of a multi-copper nitrite reductase determined by pulsed EPR (iDEER) spectroscopy. Angew Chem Int Ed Engl. 2013; 52:1990–1993. [PubMed: 23296685]
45. Georgieva ER, Roy AS, Grigoryants VM, Borbat PP, Earle KA, Scholes CP, Freed JH. Effect of freezing conditions on distances and their distributions derived from double electron electron resonance (DEER): a study of doubly-spin-labeled T4 lysozyme. J Magn Reson. 2012; 216:69–77. [PubMed: 22341208]
46. Kittell AW, Hustedt EJ, Hyde JS. Inter-spin distance determination using L-band (1–2 GHz) non-adiabatic rapid sweep electron paramagnetic resonance (NARS EPR). J Magn Reson. 2012; 221:51–56. [PubMed: 22750251] A rapid field scan methodology at L band is introduced that eliminates the modulation detection typically employed in EPR spectrometers. In addition to an improvement in overall sensitivity, the absence of instrumental line broadening from field modulation allows detection of weak dipolar interactions from spin pairs, which can be used to determine inter-spin distances. The NARS EPR instrument is available to investigators at the National Biomedical EPR Center at the Medical College of Wisconsin in Milwaukee.
47. López CJ, Fleissner MR, Guo Z, Kusnetzow AK, Hubbell WL. Osmolyte perturbation reveals conformational equilibria in spin-labeled proteins. Protein Sci. 2009; 18:1637–1652. [PubMed: 19585559]
48. Yang Z, Liu Y, Borbat P, Zweier JL, Freed JH, Hubbell WL. Pulsed ESR dipolar spectroscopy for distance measurements in immobilized spin labeled proteins in liquid solution. J Am Chem Soc. 2012; 134:9950–9952. [PubMed: 22676043] ATAM radical is introduced as a novel spin label for proteins. Immobilization of a protein containing two TAM side chains on a solid support prevented averaging of inter-spin dipolar interactions. Given the long phase memory time (T_m) of TAM, it was then possible to measure inter-spin distances via dipolar interactions at ambient rather than the usual cryogenic temperature using PD spectroscopy (DQC).
49. Jäger H, Koch A, Maus V, Spiess HW, Jeschke G. Relaxation-based distance measurements between a nitroxide and a lanthanide spin label. J Magn Reson. 2008; 194:254–263. [PubMed: 18674941]
50. Jun S, Becker JS, Yonkunas M, Coalson R, Saxena S. Unfolding of alanine-based peptides using electron spin resonance distance measurements. Biochemistry. 2006; 45:11666–11673. [PubMed: 16981726]
51. Liu CC, Schultz PG. Adding new chemistries to the genetic code. Annu Rev Biochem. 2010; 79:413–444. [PubMed: 20307192]
52. Sarver J, Silva KI, Saxena S. Measuring Cu^{2+}-nitroxide distances using double electron–electron resonance and saturation recovery. Appl Magn Reson. 2012:10. http://dx.doi.org/10.1007/s00723-012-0422-x:1-12. The authors compare inter-spin distances between Cu^{+2} and a nitroxide in a peptide determined from T1 relaxometry (echo-detected saturation recovery) and static dipolar interactions (DEER), both at low temperature. It is found that the distances measured by relaxometry can be predicted from the DEER distance distributions, and are strongly weighted toward the shortest distances. Data from relaxometry and DEER obtained at low temperature can in principle be compared with relaxometry data obtained with pulse SR at physiological temperatures to investigate the effect of freezing on structure.
53. Zhang Z, Fleissner MR, Tipikin DS, Liang Z, Moscicki JK, Earle KA, Hubbell WL, Freed JH. Multifrequency electron spin resonance study of the dynamics of spin labeled T4 lysozyme. J Phys Chem B. 2010; 114:5503–5521. [PubMed: 20361789]
54. Nesmelov Y, Thomas D. Protein structural dynamics revealed by site-directed spin labeling and multifrequency EPR. Biophys Rev. 2010; 2:91–99. [PubMed: 21687819]
55. López CJ, Oga S, Hubbell WL. Mapping molecular flexibility of proteins with site-directed spin labeling: a case study of myoglobin. Biochemistry. 2012; 51:6568–6583. [PubMed: 22809279]

This article presents a comprehensive study of the holo-, apo- and the molten globule states of myoglobin that highlights the utility of continuous wave lineshape analysis combined with osmolyte perturbation and PD spectroscopy to identify disordered regions, detect ns backbone fluctuation in ordered sequences, and identify sequence-correlated conformational flexibility on the microsecond and longer time scales. Lineshape analysis revealed a correlation between the rate and amplitude of R1 motion with extent of local packing (Figure 3a), which strongly supports a model wherein variation in R1 motion at surface sites in ordered helices reflects contributions from ns backbone fluctuations.

56. Fourme R, Girard E, Akasaka K. High-pressure macromolecular crystallography and NMR: status, achievements and prospects. Curr Opin Struct Biol. 2012; 22:636–642. [PubMed: 22959123]
57. McCoy J, Hubbell WL. High-pressure EPR reveals conformational equilibria and volumetric properties of spin-labeled proteins. Proc Natl Acad Sci USA. 2011; 108:1331–1336. [PubMed: 21205903]

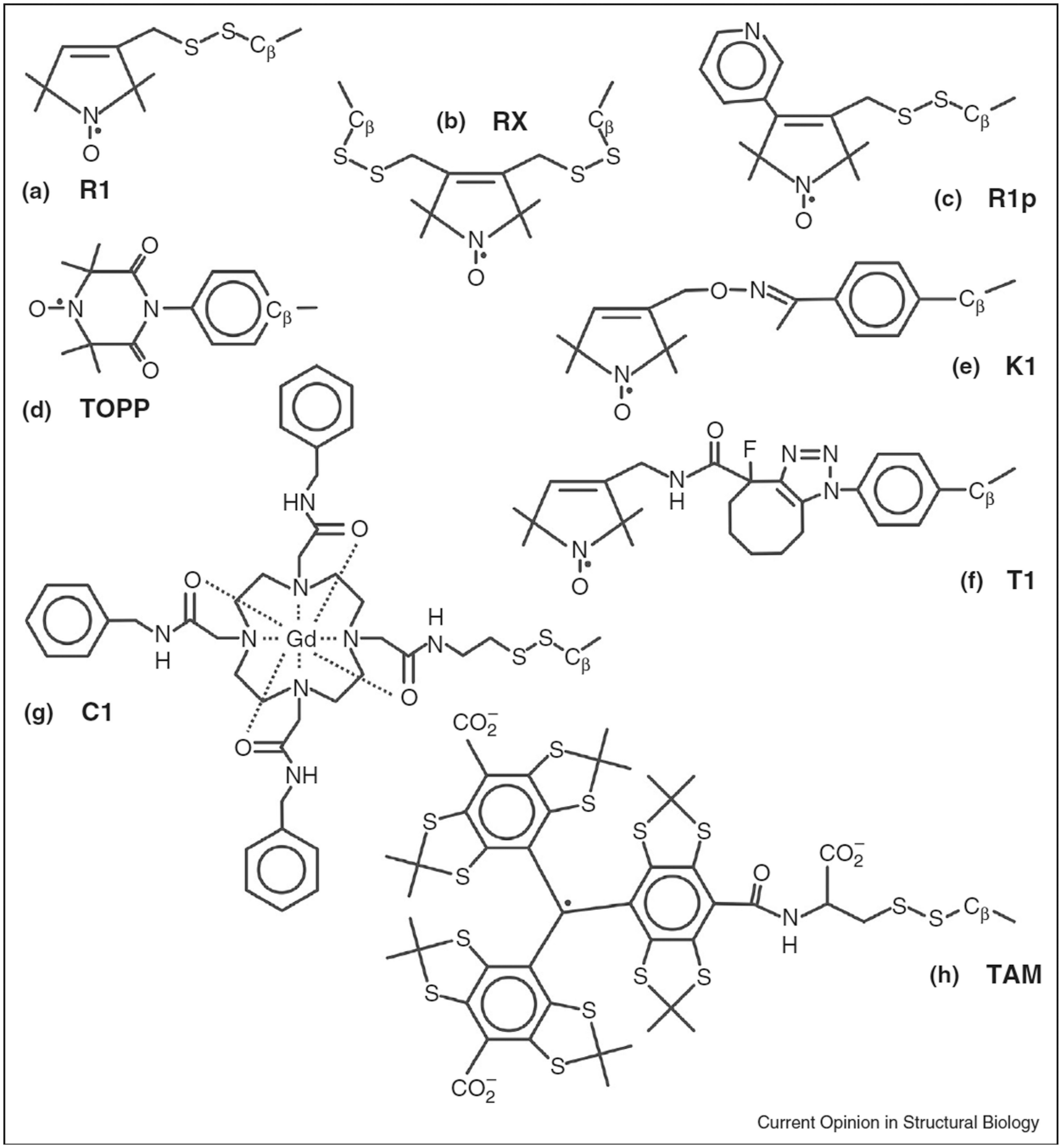

Figure 1.

Structures of paramagnetic protein labels represented as side chains. **(a)** The R1 side chain. **(b)** The cross-linking side chain RX. The cross-link can be formed between *i* and *i*± 3 or *i*± 4 cysteine residues within a regular helix, between *i* and *i*± 2 residues in a β strand, or between any elements with properly spaced cysteine residues. **(c)** The R1p side chain. **(d)** The TOPP residue introduced by peptide synthesis. Although there may be rotation about individual bonds, the nitroxide is fixed in the same spatial location, because all bonds connecting the nitroxide with the protein are collinear. **(e)** The ketoxime-linked side chain K1 generated by reaction of a p-acetyl-phenylalanine unnatural amino acid with a

hydroxylamine nitroxide reagent. **(f)** The triazole-linked side chain T1 generated by the reaction of a p-azido-phenylalanine unnatural amino acid with a strained cyclooctyne nitroxide reagent using Cu-free Click chemistry. **(g)** A disulfide-linked Gd^{3+} chelate side chain. **(h)** A disulfide-linked TAM spin label.

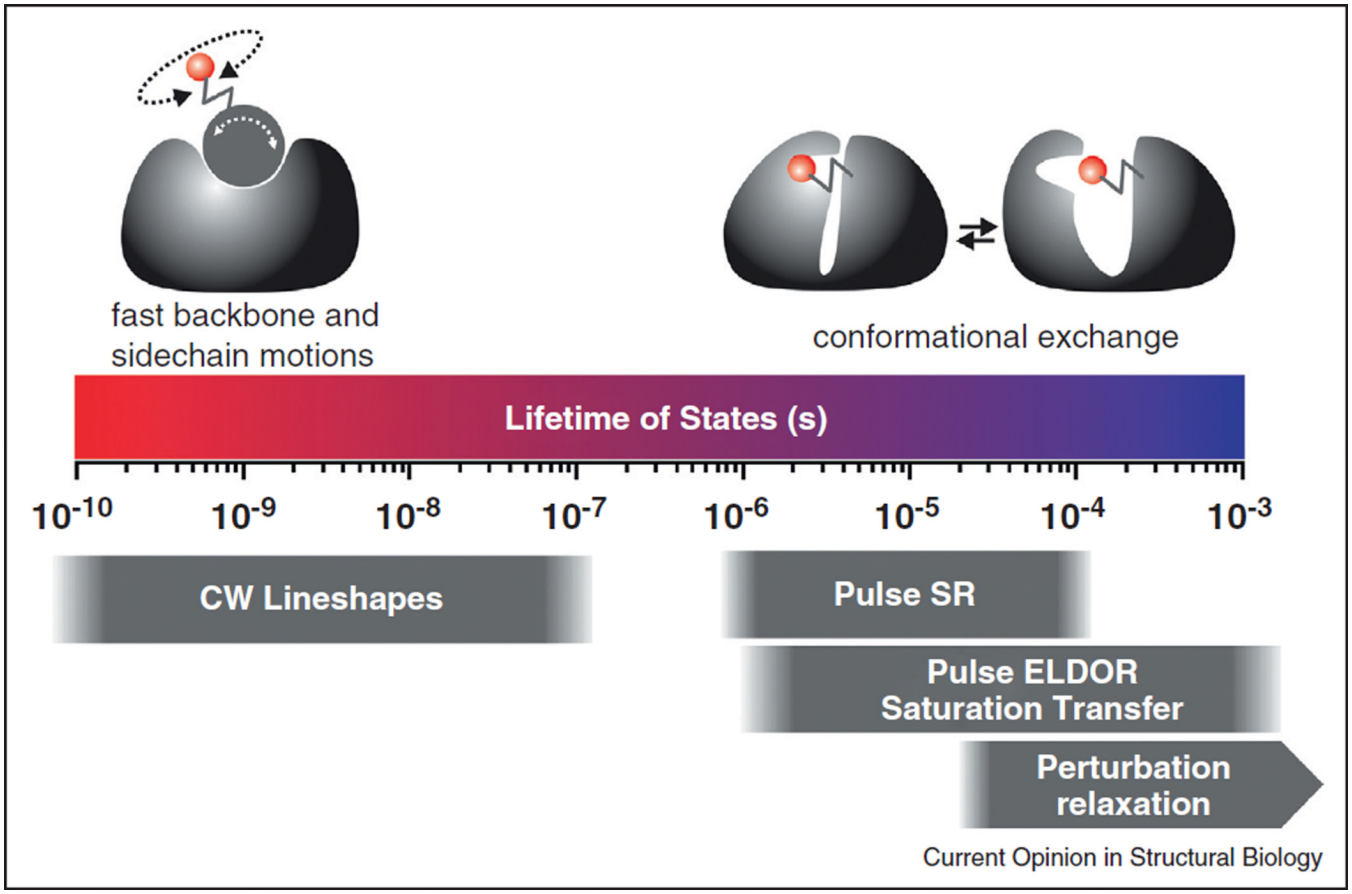

Figure 2.

Characteristic time scale (lifetime of states) for selected protein motions relative to that for X-band EPR spectroscopic methods. The panel above the time line shows cartoons illustrating backbone fluctuations and internal motions of R1 on the ns time scale (left), and conformational exchange on the μs–ms time scale (right). In each case, the red sphere represents the nitroxide of R1. Fast backbone motion adds to the internal motion of R1 on the same time scale and is thus revealed in the CW lineshape (lower panel). Conformational exchange is too slow to affect the CW lineshape, but may be revealed as resolved components in the EPR spectrum, provided that R1 is in a region where the nitroxide experiences distinct environments in each state (upper panel, right). ST-EPR, P-ELDOR, and P-SR can measure conformational exchange kinetics on the μs time scales indicated. For conformational exchange on the time scale of ms and longer, perturbation-relaxation methods are promising. Following a rapid perturbation in an experimental parameter (pressure, temperature, pH, etc.), the relaxation to a new equilibrium is monitored in real time using the EPR spectrum of a judiciously placed spin label. For commercial spectrometers with CW detection, the shortest time that can be measured by relaxation methods is limited by the 100 kHz field modulation frequency to about 50 μs, but has no upper limit.

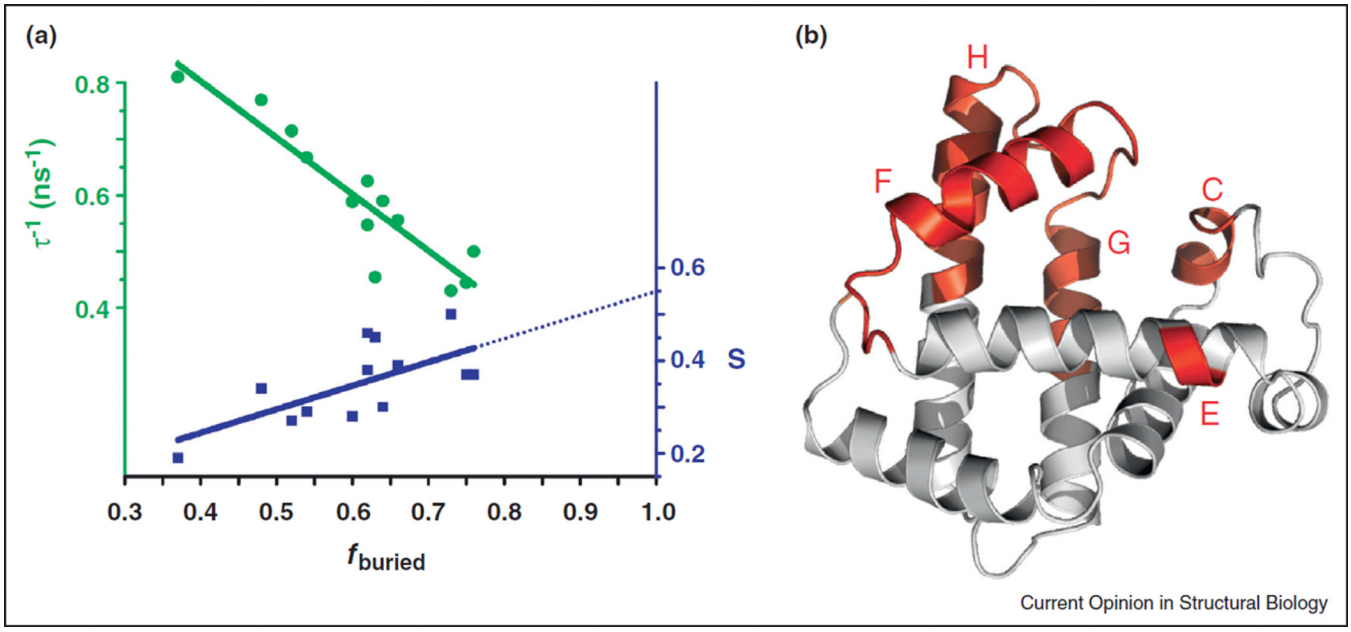

Figure 3.

Mapping backbone and conformational flexibility with SDSL-EPR. **(a)** The rate (inverse correlation time, τ^{-1}) and order parameter (S) for R1 motion at solvent-exposed helix surface sites in myoglobin are plotted versus the fraction of buried surface area (f_{buried}) for the helix segment containing R1; f_{buried} is proportional to the number of contacts the segment makes with the fold. The regular decrease in rate and increase in order of R1 motion with increasing f_{buried} is consistent with a plausible model in which increased contact of a segment damps motion which is reflected in R1 dynamics. This result strongly supports the contention that the variation in R1 motion from site-to-site at solvent-exposed sites reflects backbone motion rather than local side chain interactions. **(b)** Regions in conformational exchange (μs or longer, red ribbon), as detected by resolved components in the R1 spectrum and the response to osmotic perturbation, are mapped onto a structural model of myoglobin. The regions identified correspond closely with those obtained by NMR methods [55••]. The figures are adapted from [55••].

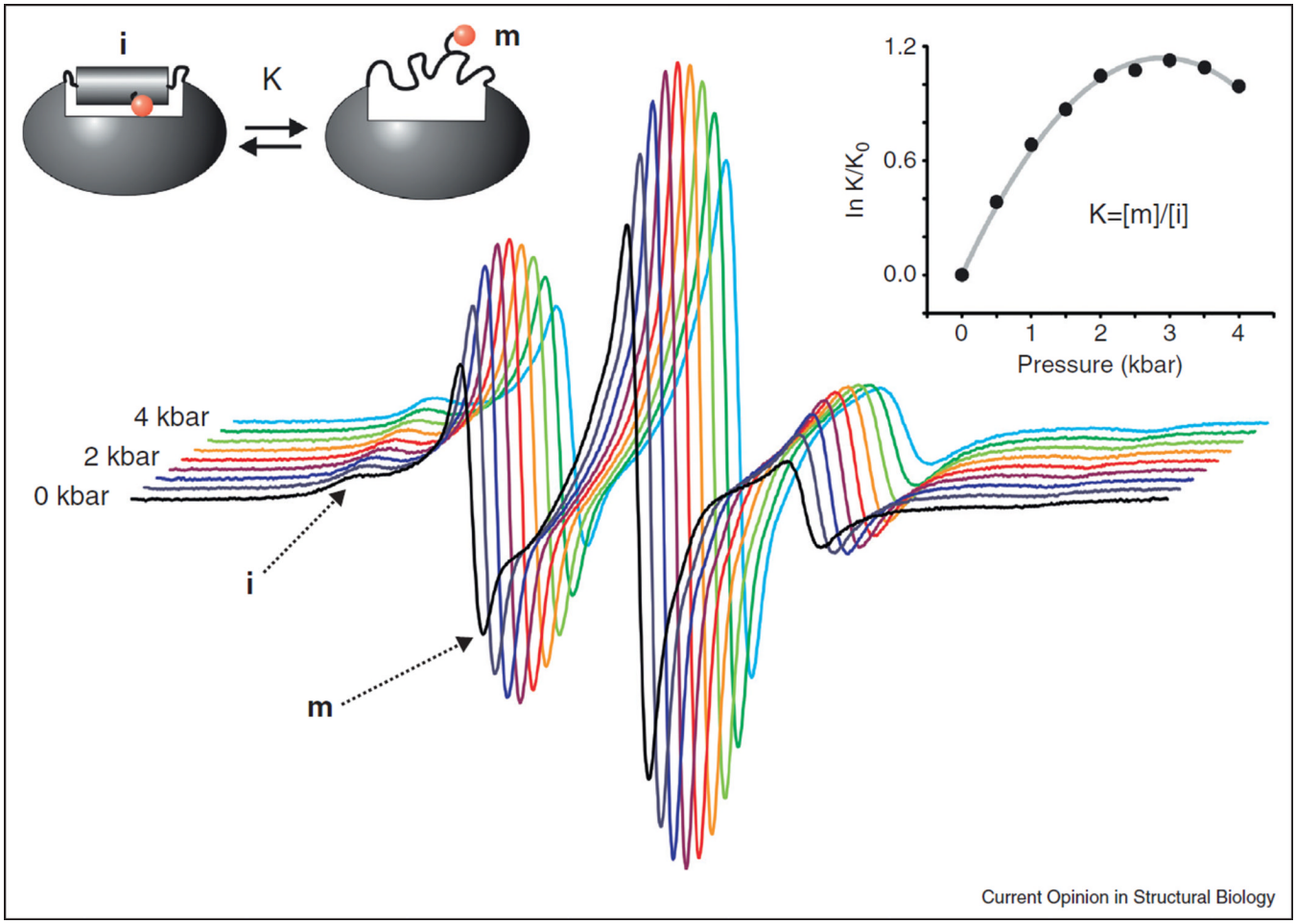

Figure 4.

Pressure dependence of a protein conformational equilibrium detected by SDSL-EPR. The stack plot of EPR spectra are for the A46R1 mutant of T4 lysozyme as a function of pressure. The two resolved spectral components *i* and *m* arise from equilibrium between a folded conformation (*i*) and a locally unfolded state (*m*) as illustrated schematically in the cartoon where the colored sphere represents the spin label. The apparent equilibrium constant, K, determined from the spectra, is a function of pressure as shown in the plot of $\ln[K(P)/K_o]$ versus pressure. The solid trace is a fit of the data to a model wherein the two conformations have different partial molar volumes as well as compressibilities. The figure is adapted from McCoy and Hubbell [57]. The relative populations of *i* or *m* could be directly monitored in time at a fixed field following a pressure jump.